Annals of Nuclear Energy 172 (2022) 109082

Contents lists available at ScienceDirect

Annals of Nuclear Energy

journal homepage: www.elsevier.com/locate/anucene

A new methodology for thermal analysis of geological disposal of spent nuclear fuel using integrated simulations of gamma heating and finite element modeling

Peter Jansson [a,*], Peter Renström [b], Jan Sarnet [c], Anders Sjöland [c]

[a] Uppsala University, Sweden
[b] Advanced Engineering Computation (AEC AB), Sweden
[c] Swedish Nuclear Fuel and Waste Management Company (SKB AB), Sweden

ARTICLE INFO

Article history:
Received 16 September 2021
Received in revised form 3 March 2022
Accepted 15 March 2022
Available online 22 March 2022

Keywords:
Thermal model
Gamma heating
KBS-3
Geological disposal
Nuclear fuel
Decay heat
Temperature
Monte Carlo
Geant4
FEM

ABSTRACT

A new methodology is illustrated, where the evolution of temperature in a geological disposal system for spent nuclear fuel is estimated by integrated calculations of a spatially distributed gamma heating source with conventional finite element thermal transport modeling. A case with one canister loaded with fuel assemblies with a cooling time of 30 years in a KBS-3 type repository illustrates the methodology. For this particular case, the effect of including distributed gamma heating rate in the modeling has a small impact on the temperature distribution compared to the conventional case of heat generated locally in the canister, resulting in a small decrease of the maximum temperature in the canister. A large proportion of gamma heating occurs inside the outer boundary of the copper canister for this case. Other potential consequences of radiation escaping the canister are discussed.

1. Introduction

In final geological disposal of spent nuclear fuel, knowledge of the development of temperatures are important for the safety and integrity of the fuel assemblies, barriers and buffers protecting the environment from the radiotoxicity of the fuel. Modeling of the temperature distribution in the repository is typically performed using nominal values of decay heat rate from the fuel assemblies. The decay heat rates are typically used as linear sources of heat (Ikonen, 2020), representing the canister or the fuel assemblies in the canister, depending on the level of detail.

The decay heat rate from the nuclear fuel originates from decay of radioactive material inside it, see e.g. (Tobias, 1980). Temperature increase of the fuel and its surroundings is a result of energy transferred from the radiation that is emitted in the radioactive decay to kinetic energy of electrons and atoms.

In this work, the effect on modeled temperature distributions in a KBS-3 type deep geological repository, see e.g. (Design and production of the KBS-3 repository, 2010), using a heat source that is more distributed compared to a linear heat source for the first time to the authors' knowledge. By using Monte Carlo methods to transport gamma radiation emitted from the nuclear fuel and calculating where it deposits its energy, we simulate distributed gamma heating sources that are typical for one example of a canister loaded with used nuclear fuel.

We have focused on gamma heating since they have the potential to significantly heat structures outside the fuel pellets. Alpha and beta particles will to a large degree stop inside the fuel and the number of neutrons emitted per time is significantly smaller than the number of gamma particles per time at the cooling times of around 30 years studied here. Significant amounts of energy are escaping through neutrinos with extremely low cross sections for interaction with matter, thus not contributing much to heating of the repository.

Using the calculated distributed heat source, the temperature distribution was modelled by the heat diffusion equation and Stefan-Boltzmann's law of heat radiation which was solved using a finite element model. The thermal modeling was used in some

* Corresponding author.
E-mail address: peter.jansson@physics.uu.se (P. Jansson).

https://doi.org/10.1016/j.anucene.2022.109082
0306-4549/

chosen thermal load cases in one example of canister configuration including one nuclear fuel type.

The paper is structured as follows: the second section describes the gamma heating model in section 2.1 and results from using the heating model in 2.2. The third section describes the thermal model in section 3.1 and results of using the thermal model in 3.2, including results from the gamma heating model. Conclusions are listed in section 4 and the final section discusses the work and a future outlook. All radial distances mentioned in the paper refers to the center of the canister.

2. Gamma radiation heating

In the process of radioactive decay, the emitted radiation and particles carry with it energy that is transferred to matter upon interaction. The deposited energy will increase the temperature at and around the point of interaction. In management of nuclear fuel, the energy of emitted radiation per time unit is often referred to as decay heat which in a strict sense is not correct since the heat is a later result of increasing temperature wherever the radiation deposits its energy.

In this section, we establish a model of such heating from gamma radiation emitted from spent nuclear fuel in a copper canister in a KBS-3 type of deep geological repository (Design and production of the KBS-3 repository, 2010) and present results from that modeling.

2.1. Gamma heating model description

The majority of heating in the fuel assemblies and immediate structures originates from electrons from beta decay. Due to the low mean free path of alpha and beta particles, they deposit their energy relatively close to their point of origin. The emitted gamma radiation however has a smaller probability of interaction and will deposit their energy further away.

For the purpose of calculating the heating source due to gamma radiation emitted from the spent nuclear fuel, one canister with its copper shell, iron cast insert and the surrounding bentonite buffer and granite bedrock was modelled using the Geant4 Monte Carlo framework version 10.02 (Agostinelli et al., 2003). Nominal values, e.g. a symmetrically placed canister in the deposition hole, based on information on geometry and material properties from (Design, production and initial state of the canister, 2010; Design, production and initial state of the backfill and plug in deposition tunnels, 2010) were used.

For the purpose of this work, dry clay was modeled in the calculations as MX-80 clay using information from (Design, production and initial state of the backfill and plug in deposition tunnels, 2010). Although it is expected that the clay will be saturated with water after a relatively short period of time, the content of water has a minor impact on the attenuation of gamma radiation compared to the other constituents of the clay.

Twelve nuclear fuel assemblies of boiling water (BWR) type Svea-96S, manufactured by Asea Atom AB, were placed in the iron cast insert in the model. Fig. 1 displays the geometry as modeled by Geant4.

At the cooling times considered here, around 30 years, the gamma-ray energy spectrum is dominated by emissions from decay of ^{137}Cs and ^{154}Eu, see e.g. (Jansson, 2016). Fig. 2 displays a typical energy spectrum of emitted photons for a BWR assembly at a cooling time of 30 years after the end of irradiation. We have used the dominating spectral energies of 662 keV and 1274 keV from ^{137}Cs and ^{154}Eu in the calculations.

For each gamma-ray energy, the emitted gamma-ray and following scatterings and electron transports et.c. were tracked in the Geant4 framework. Gamma particles were emitted homogeneously over each rod in the fuel assembly from a plane on the midplane of the geometry. The energy deposited, per emitted gamma particle, in a mesh with 1 cm^3 voxels was calculated. Post-processing of the results was performed by summing the mesh over the z direction (axial direction). Due to axial symmetry, this procedure results in a deposited energy at z = 0, per emitted particle and fuel rod, which would be the same as having emissions distributed over z and calculating the energy deposition in the voxel at z = 0. Using a planar source at z = 0 and summing the meshed energy depositions over z is computationally more efficient compared to using a 3D source distribution and calculating the energy deposition in one voxel at z = 0.

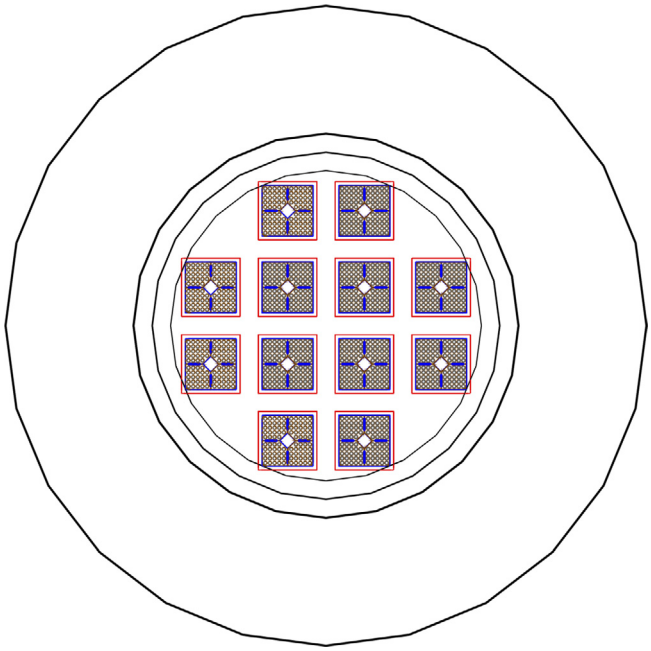

Fig. 1. A sketch of the Geant4 geometrical model used in the calculations. Here, the case with twelve BWR assemblies of the Svea-96S type is displayed, viewed from the top. The circular shapes representing the insert, copper canister and buffer are seen as jagged due to a limitation in the Geant4 visualization engine but are circular in the model.

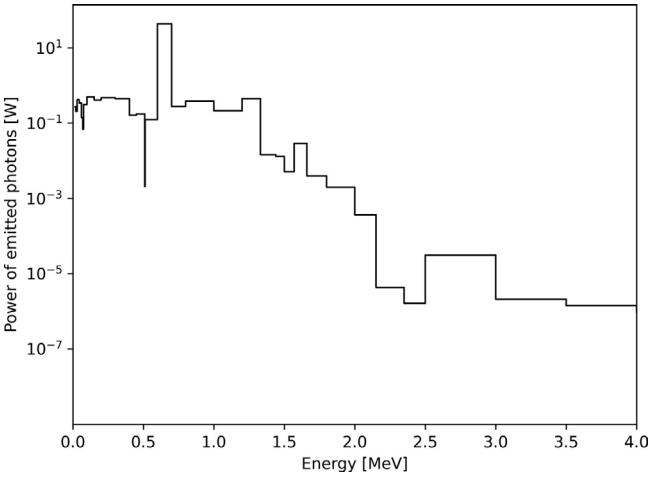

Fig. 2. An energy spectrum of photon power (emitted energy per time unit) emitted in a BWR nuclear fuel assembly after 30 years of cooling time, calculated using ORIGEN-S. The fuel had 3% initial enrichment of ^{235}U and a burnup of 40 GWd/tU. Data from (Jansson 2002).

The emission energy spectrum in units of emitted photons per energy and time of the fuel assembly together with the deposited energy per emitted particle in the voxels at (x, y, z = 0) allowed to calculate a map of the energy deposition per unit of time in the (x, y) plane in the system, i.e. the heating rate.

In the thermal modeling which is described in a later section, a one-dimensional system is used. Therefore, the energy deposition per unit time was averaged over the azimuthal angles of 0–360°, at a specific radial distance.

2.2. Gamma heating results

Due to the size of the calculated mesh with energy deposition, only a selection or slices of it can be efficiently presented here. The full set of calculated energy depositions can be found in reference (Jansson, 2017).

Fig. 3 displays a map of the spatial energy deposition at the canister's mid-plane calculated for the Svea-96S BWR case considered here. It can be noticed that proton rich materials in the system are, as expected, subjected to a relatively high energy deposition from emitted gamma radiation, compared to other materials.

Using the azimuthal averaging, the radial profile of gamma radiation power in the system was calculated. The results are displayed in Fig. 4. The gamma power part emitted by ^{137}Cs and ^{154}Eu was estimated to represent about 95 % of the total gamma power emission for the case considered here. Therefore, the gamma emission energy spectrum was approximated to two energy groups with a corresponding two-group approximation for the spatial heating distribution; 0 to 0.9 MeV corresponding to ^{137}Cs and 0.9 to 12 MeV corresponding to ^{154}Eu. The amount of energy deposited outside the canister was less than 0.2 % of the energy deposited inside the canister, see ref. (Renstrom, 2019a) for details.

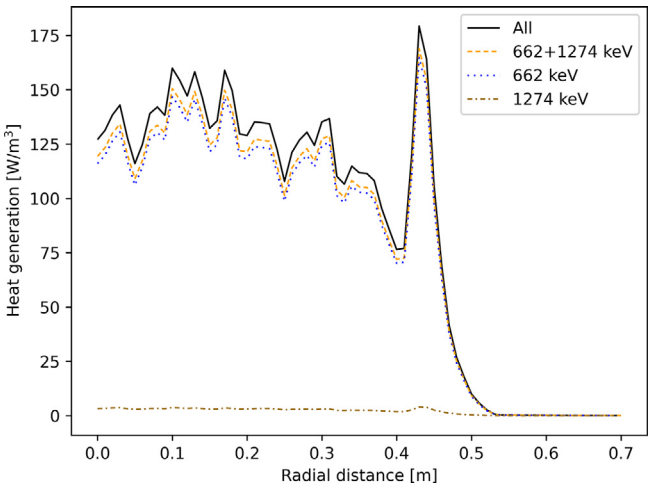

Fig. 4. Deposited gamma radiation power in the system with Svea-96S fuel assemblies, averaged over 360° for each radial distance. The total gamma emission power is denoted by "All", the contribution from the sum of ^{137}Cs and ^{154}Eu by "662 + 1274 keV", from ^{137}Cs by "662 keV" and from ^{154}Eu by "1274 keV".

3. Thermal evolution

The maximum temperature at the outer surface of the copper canister must be limited according to requirements for the KBS-3 type deep geological repository (Design, production and initial state of the canister, 2010) (presently below 100 ℃). In this context, it is therefore of interest to study how distributed heating from gamma radiation possibly could affect the canister surface temperature.

Due to the high thermal conductivity of copper, it can be assumed that the temperature variation on and exterior of the copper shell is small, especially in the circumferential direction (Ikonen, 2020). This motivated the choice of a simplified one-dimensional, radial, computational model which is described in this section together with temperature results from a sensitivity analysis consisting of a number of comparative heat load distributions.

3.1. Thermal model description

The energy distribution per unit of time calculated in the gamma heating model for the fuel type BWR Svea-96S, see Fig. 3, was used as heat load in a one-dimensional time-dependent thermal finite element model located at the canister's midplane, assuming cylindrical symmetry in the near-field and spherical

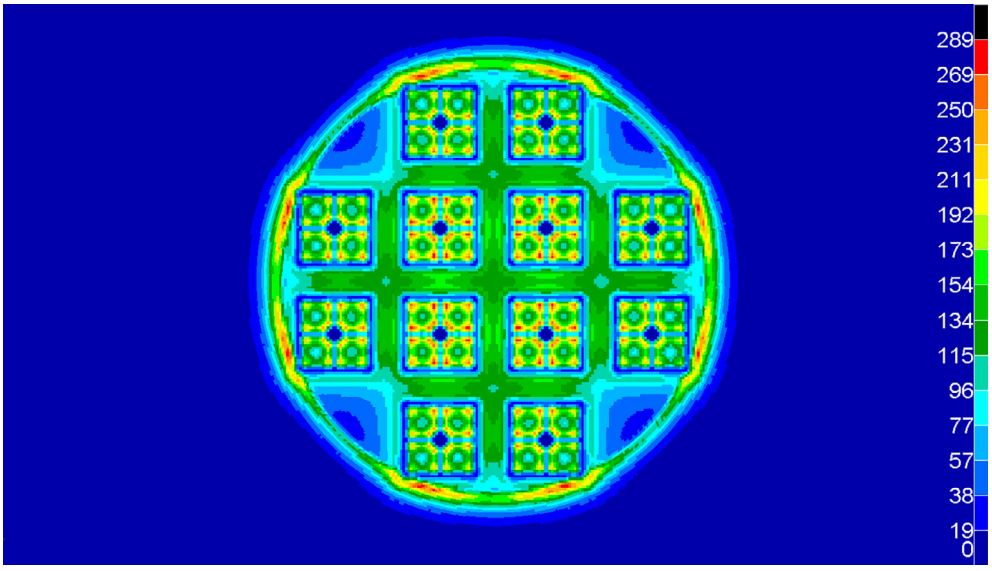

Fig. 3. A spatial map of volumetric gamma heat generation [W/m^3] from radiation emitted homogeneously over the fuel pellets in the Svea-96S fuel assemblies in the canister.

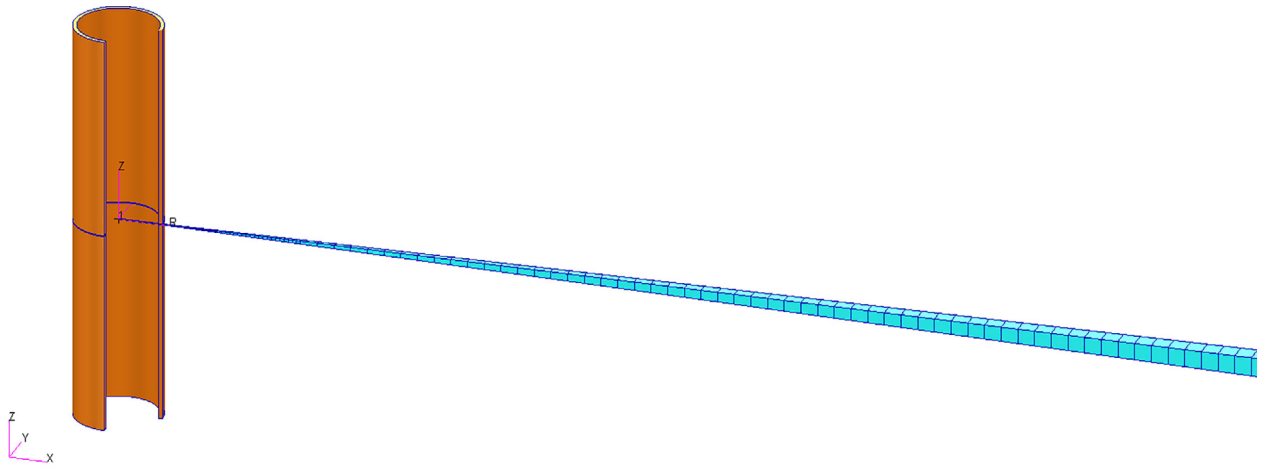

Fig. 5. Thermal FE-model (blue). The copper shell cylinder (brown) is not part of the FE-model, but is shown as a reference. Used with permission from reference (Renstrom, 2019a).

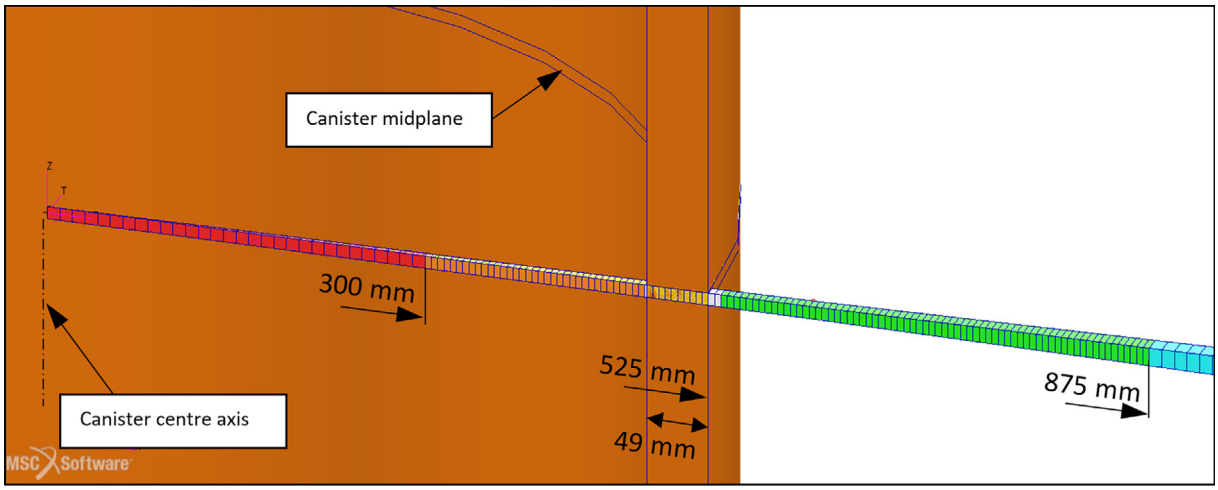

Fig. 6. Thermal FE-model, detail at canister. Red = canister internals with heat load A in Table 2, orange = canister internals, yellow = copper shell, green = buffer, blue = rock, white = inner and outer gap at copper shell, brown = copper shell shown as a reference. Used with permission from reference (Renstrom, 2019a).

symmetry in the far-field (Renstrom, 2019a, Renstrom, 2019b) (see Figs. 5 and 6). The finite element model, built in MSC.Patran with the MSC.Nastran solver (MSC 2021), was used to solve the heat diffusion equation.

$$\nabla^2 T + \frac{\dot{q}}{k} = \frac{1}{a}\frac{\partial T}{\partial t}$$

where ∇ is the nabla vector differential operator, T is temperature, $\dot{q}$ is heat rate per volume, k is thermal conductivity, α is thermal diffusivity and t is time. See, e.g., reference (Incropera and DeWitt, 2006). Heat radiation was assumed over the gas-filled gaps on both sides of the copper shell according to Stefan Boltzmann's law.

$$\frac{dQ}{dt} = \varepsilon\sigma\left(T^4 - T_0^4\right)A$$

where Q is heat, ε is emissivity, σ is Stefan-Boltzmanns' constant, T_0 is ambient surface temperature and A is surface area. Heat transfer by convection in the gas-filled gaps was neglected.

Due to the thermal model's one-dimensional nature, neither the canister's internals nor the distributed heat load could be modeled in detail. Therefore, the physical properties such as thermal conductivity and heat capacity for fuel assemblies, tubes and insert were averaged by weighting them by their relative sectional properties in accordance with reference (Ikonen, 2020). The thermal conductivity of the buffer was chosen to be 1.0 W/mK, but it should be noted that this value varies significantly with the water saturation of the bentonite (Renstrom, 2019b). The physical properties used in the thermal FE-model are shown in Table 1.

The total heat power for one canister was chosen to 1705 W as an initial value at a cooling time of 33 years, with a time-dependent decay curve according to reference (Ikonen, 2020).

Table 1
Physical properties used in the thermal FE-model (Renstrom, 2019a).

Material	k (W/(mK))	ρc_p (MJ/(m^{3}K))	ε (emissivity)
canister internals	23.6	2.7	–
nodular iron	–	–	0.6
argon (inner gap)	0.022	$8.58{\cdot}10^{-4}$	–
copper	390	3.45	0.1/0.3 in-/outside
air (outer gap)	0.03	$8.8{\cdot}10^{-4}$	–
buffer	1.0	2.4	0.8
rock	2.55	2.12	–

Table 2
Load cases used in this study. Load A = part of residual heat load generated inside radius 300 mm, load B = part of residual heat load emanating from deposited gamma radiation.

Load Case no	Load A	Load B	Load B distribution	Load B location
1	100 %	0 %	–	–
2	73 %	27 %	"662 + 1274 keV" in Fig. 4	"662 + 1274 keV" in Fig. 4
3	73 %	27 %	uniform	in copper shell only
4	73 %	27 %	uniform	in 50 mm inner torus of buffer only
5	73 %	27 %	uniform	in buffer only

In this study, five load cases of different heat load distributions were defined in order to investigate the heat load distribution's influence on the temperature field close to the canister. The defined load cases are listed in Table 2. The first load case has the entire residual heat uniformly generated inside radius 300 mm corresponding to the red part of the FE-model in Fig. 6, similar to reference (Ikonen, 2020). For the second load case, we assume a typical fraction of the total heat rate from the decays of ^{137}Cs and ^{154}Eu of 27%, see e.g. reference (Jansson, 2002). The gamma heating simulations in subsection 2.2 show where this heat rate is distributed. The rest of the residual heat, 73 %, is assumed to be generated in the conventional way as in load case 1. Load cases 3, 4 and 5 should be seen as comparative sensitivity analyses, in which 27 % of the residual heat is generated in the copper shell, a narrow torus of buffer and the whole buffer, respectively.

3.2. Thermal modeling results and temperature distributions

The surface temperature at the midplane of a single canister with the residual heat load modelled in the conventional way without regards to distributed gamma heating, from the time of emplacement in the final repository up to 20 years thereafter, is shown as load case 1 in Fig. 7. The results for load case 1 is in Fig. 7 also compared to results from load cases 2 to 5 in which the heat load from deposited gamma radiation is modelled in different spatial distributions. Analogously, the calculated temperature in the buffer at 0.75 m from the canister centre axis is shown in Fig. 8.

In Figs. 9-11, the calculated temperature at midplane for a single canister as a function of radial distance from the centre axis is shown for load case 1 to 5 at different times after emplacement in the final repository. The calculated surface temperatures at 0.5, 3 and 10 years after time of emplacement in the final repository are tabulated in Table 3. In this work, we have not studied uncertainties of the temperatures calculated using our approach but the reader can find a sensitivity study of how variation of material properties, gap sizes et.c. may influence the surface temperature of the canister in reference (Renstrom, 2019b).

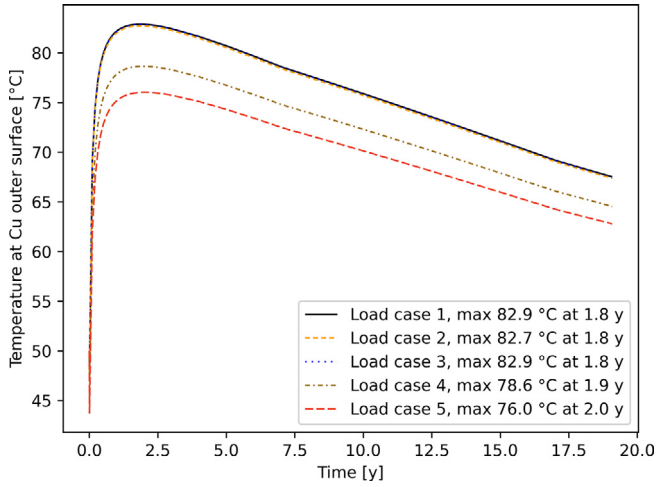

Fig. 7. Surface temperature at midplane for a single canister for load cases 1 to 5. Load cases 1 to 3 virtually overlap.

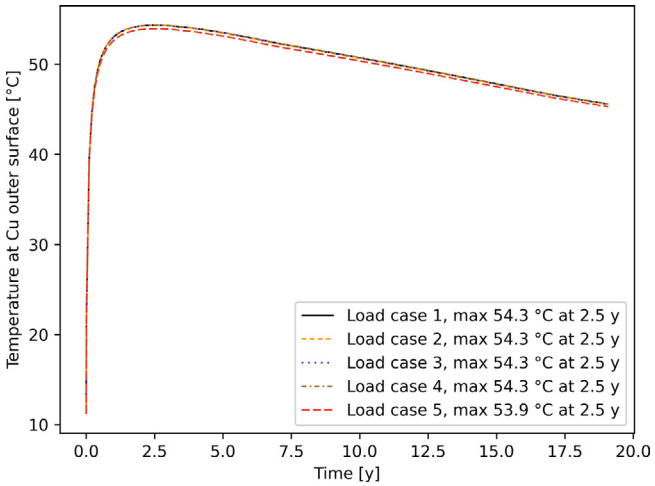

Fig. 8. Buffer temperature at midplane 0.75 m from centre for a single canister for load cases 1 to 5. Load cases 1 to 4 virtually overlap.

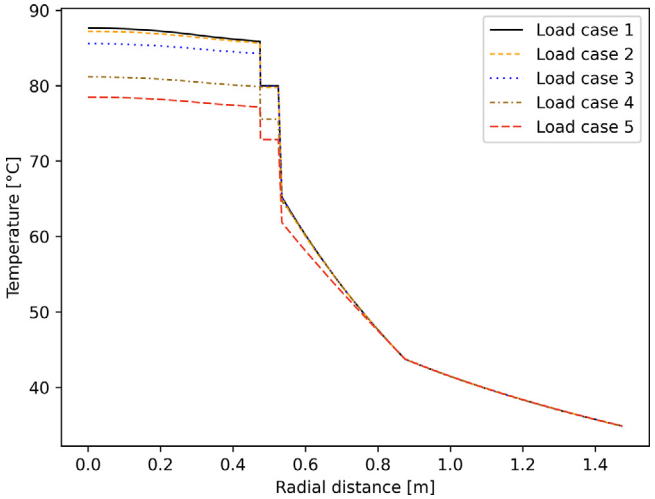

Fig. 9. Calculated temperature at the midplane of a single canister as a function of radial distance from the centre axis for load case 1 to 5 at 0.5 years after emplacement in the final repository.

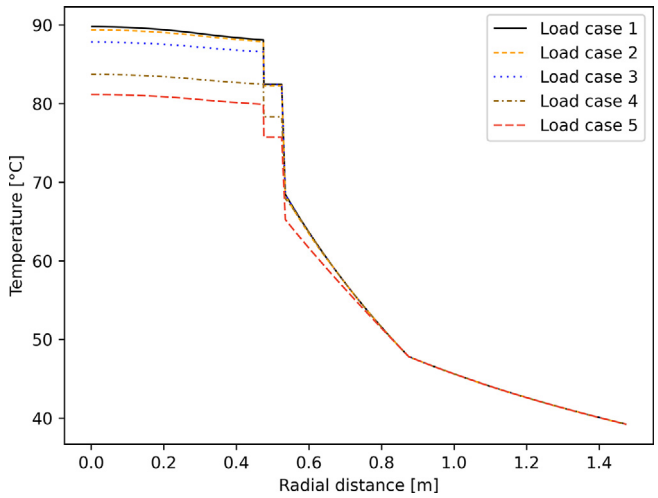

Fig. 10. Calculated temperature at the midplane of a single canister as a function of radial distance from the centre axis for load case 1 to 5 at 3 years after emplacement in the final repository.

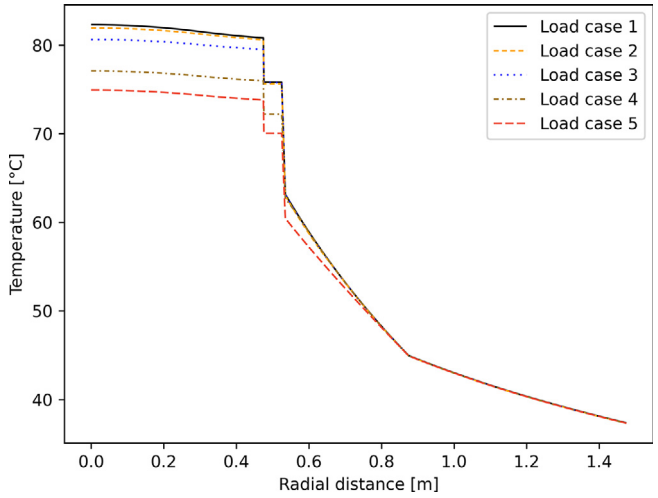

Fig. 11. Calculated temperature at the midplane of a single canister as a function of radial distance from the centre axis for load case 1 to 5 at 10 years after emplacement in the final repository.

Table 3
Calculated surface temperature at the midplane for a single canister at different times after deposition in the final repository for load cases 1 to 5.

Load Case no	0.5 years	3.0 years	10 years	Maximum
1	80 °C	82 °C	76 °C	83 °C
2	80 °C	82 °C	76 °C	83 °C
3	80 °C	82 °C	76 °C	83 °C
4	76 °C	78 °C	72 °C	79 °C
5	73 °C	76 °C	70 °C	76 °C

4. Conclusions

Based on the modeling framework and the for the example used here with a canister loaded with twelve Svea-96S fuel assemblies with a cooling time of about 30 years, we can conclude that;

1. A relatively small amount of gamma heating occurs outside the copper canister.
2. The results from the thermal model for load cases 1, 2 and 3 show that the evolution of canister surface temperature over a time-scale of years is practically independent of the spatial distribution of the heat load inside the canister. However, in case a significant fraction of heat is produced from sources outside the canister, as in load case 4 and 5, the canister surface temperature will be lower. Thus, the effect from distributed gamma heating on the canister surface temperature over a time-scale of years will be low as long as the amount of gamma energy reaching outside the canister is low compared to the total decay heat load.
3. For this particular case, the effect of including distributed gamma heating rate in the modeling has a small impact on the temperature distribution, resulting in a small decrease of the maximum temperature in the canister compared to conventional modeling approaches with line heat sources.

5. Discussion and outlook

It should be noted that the conclusions listed above are representative of the case considered here. Other conclusions might be reached when, for instance, nuclear fuel assemblies with shorter cooling time are placed in the canister. Such assemblies have a relatively higher average energy of emitted gamma radiation which might penetrate and escape the canister more compared to the case here.

Since distributed gamma heating can be regarded as a local phenomenon close to the canister, the comparative temperature calculations in this report was made for a fictitious case with only one canister emplaced in the deep repository environment. In KBS-3, the decay heat from all other surrounding canisters will contribute to give a higher canister temperature a few years after emplacement, as reported by (Ikonen, 2020; Hokmark et al., 2010).

It is anticipated that pressurized water reactor (PWR) fuel assemblies, that have a more dense fuel lattice compared to BWR fuel assemblies, may have an effect on the penetration capability of the gamma radiation and hence may influence the results presented for the BWR case studied here.

The modeling framework used here is based on the heat diffusion equation and Stefan-Boltzmann's law of heat radiation regarding the thermal modeling and using Monte Carlo calculations for the gamma radiation transport. No special cases, such as a canister misalignment or sensitivities in thermal conductivity of e.g. the clay buffer were considered. We envision however, that such sensitivity studies can be performed based on this framework.

Neutrons emitted from the spent nuclear fuel, e.g. from spontaneous fission of ^{244}Cm, have the potential to damage chemical structures and to react with the nuclei in the bentonite system that contains mostly light elements enabling good moderation of the neutrons. For example the properties of the clay buffer may change over longer periods of time due to neutron irradiation. We are currently researching such effects using the same Geant4 Monte Carlo framework used in this study, in addition to gamma radiation induced effects.

CRediT authorship contribution statement

Peter Jansson: Conceptualization, Methodology, Software, Investigation, Data curation, Visualization, Writing – original draft, Writing – review & editing. **Peter Renström:** Conceptualization, Methodology, Software, Investigation, Data curation, Visualization, Writing – original draft, Writing – review & editing. **Jan Sarnet:** Project administration, Funding acquisition, Writing – review & editing. **Anders Sjöland:** Methodology, Project administration, Funding acquisition, Writing – review & editing.

Declaration of Competing Interest

The authors declare that they have no known competing financial interests or personal relationships that could have appeared to influence the work reported in this paper.

Acknowledgements

The Monte Carlo computations were enabled by resources provided by Swedish National Infrastructure for Computing (SNIC) at Uppsala Multidisciplinary Center for Advanced Computational Science (UPPMAX), National Supercomputer Centre at Linköping University (NSC) and High Performance Computing Center North (HPC2N), partially funded by the Swedish Research Council through grant agreement no. 2018-05973, under projects SNIC 2017/1-147, uppstore2017035, SNIC 2018/3-145, SNIC 2019/3-160, uppstore2018067 and SNIC 2020/5-253.

The authors acknowledge fruitful discussions and ideas generated by Mikael Jonsson with the Swedish Nuclear Fuel and Waste Management company.

References

Ikonen, K.; "Temperatures Inside SKB and Posiva Disposal Canisters for Spent Fuel"; Posiva SKB Report 12; ISSN 2489-2742; SKB ID 1495080; Posiva ID RDOC-105016; Available from: https://www.skb.se/publikation/2497605; 2020.

Tobias, A., 1980. Decay heat. Prog. Nucl. Energy 5 (1), 1–93. https://doi.org/10.1016/0149-1970(80)90002-5.

"Design and production of the KBS-3 repository"; SKB Report No. TR-10-12; Available from: http://www.skb.com/publication/2167363/TR-10-12.pdf; 2010.

Agostinelli, S. et al., 2003. "Geant4—a simulation toolkit, "Nuclear Instruments and Methods in Physics Research Section A: Accelerators. Spectrometers, Detectors and Associated Equipment 506 (3), 250–303. https://doi.org/10.1016/S0168-9002(03)01368-8.

"Design, production and initial state of the canister"; SKB Report No.: TR-10-14; Available from: https://skb.se/upload/publications/pdf/TR-10-14.pdf; 2010.

"Design, production and initial state of the backfill and plug in deposition tunnels"; SKB Report No. TR-10-16. Available from: https://skb.se/upload/publications/pdf/TR-10-16.pdf; 2010.

Jansson, P., Tobin, S., Liljenfeldt, H., Fugate, M., Favalli, A., Sjöland, A., 2016. Axial and azimuthal gamma scanning of nuclear fuel - implications for spent fuel characterization Available from: Journal: Journal of Nuclear Materials Management 45 (1).

Jansson P.; "Studies of Nuclear Fuel by Means of Nuclear Spectroscopic Methods"; Publisher: Acta Universitatis Upsaliensis; Comprehensive Summaries of Uppsala Dissertations from the Faculty of Science and Technology 714; ISBN: 91-554-5315-5; Available from: http://urn.kb.se/resolve?urn=urn:nbn:se:uu:diva-2057; 2002.

Jansson P.; "Results from Geant4 calculations of energy deposition from gamma- and neutron radiation emitted from selected cases of used boiling water reactor nuclear fuel assemblies in a KBS-3 type deep geological repository"; Available from: http://urn.kb.se/resolve?urn=urn:nbn:se:uu:diva-317843 ; 2017.

Renström, P; "Numerical Study of the Influence from Deposited Gamma Radiation Energy on Canister Temperature in the Final Repository"; SKB Report No. R-19-26; Svensk Kärnbränslehantering AB; Available from: https://www.skb.se/publikation/2496406/R-19-26.pdf; 2019a.

Renström, P; "Beräkningar av temperaturen i kopparhöljet och bufferten i förenklade parameterstudier"; SKB Report No. R-19-27; Svensk Kärnbränslehantering AB; Available from: https://www.skb.se/publikation/2496460/R-19-27.pdf; 2019b.

MSC Software Corporation, 5161 California Ave. Suite 200, Irvine, CA 92617, USA; Phone +17145408900; https://www.mscsoftware.com/ (accessed 2021-03-31); 2021.

Incropera, F., DeWitt, D., 2006. Fundamentals of Heat and Mass Transfer. John Wiley & Sons.

Hökmark, H; Lönnqvist, M; Fälth, B; "Thermal, Mechanical, Thermo-Mechanical and Hydro-Mechanical Evolution of the Rock at the Forsmark and Laxemar Sites"; Report TR-10-23; Svensk Kärnbränslehantering AB; Available from: https://www.skb.se/publikation/2033578/TR-10-23.pdf; 2010.